Science of the Total Environment 905 (2023) 166909

Contents lists available at ScienceDirect

Science of the Total Environment

journal homepage: www.elsevier.com/locate/scitotenv

Species-dependent uptake of gadolinium in *Chlamydomonas reinhardtii* algae

Karolin Sommer [a], Sarah Reuter [b], Matthias Elinkmann [a], Alexander Köhrer [a], C. Derrick Quarles Jr. [c], Michael Hippler [b,d], Uwe Karst [a,*]

[a] Institute of Inorganic and Analytical Chemistry, University of Münster, Corrensstr. 48, 48149 Münster, Germany
[b] Institute of Plant Biochemistry and Biotechnology, University of Münster, Schlossplatz 7-8, 48143 Münster, Germany
[c] Elemental Scientific, Inc., 7277 World Communications Dr., Omaha, NE 68022, United States
[d] Institute of Plant Science and Resources, Okayama University, Kurashiki, Okayama 710-0046, Japan

HIGHLIGHTS

- Interaction of Gd-based contrast agents (GBCAs) with *C. reinhardtii* algae is studied.
- Single cell ICP-MS analysis: uptake in algae for Gd^{3+} and linear GBCAs
- Total Gd analysis: more Gd in macromolecular cell structures than in the lysate
- No intact linear GBCAs detected in cell lysate via HILIC-ICP-MS.
- No uptake of macrocyclic GBCAs into the algae cells

GRAPHICAL ABSTRACT

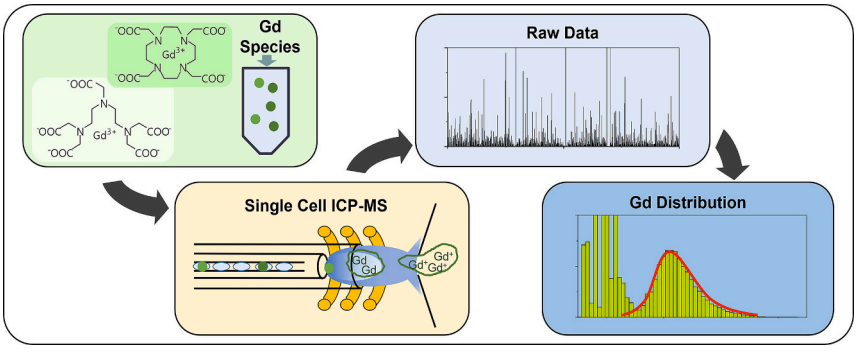

ARTICLE INFO

Editor: Damià Barceló

Keywords:
Inductively coupled-plasma mass spectrometry
Gadolinium-based contrast agents
Speciation analysis
Single cell analysis

ABSTRACT

Single cell-inductively coupled plasma-mass spectrometry (sc-ICP-MS) was used in this study as a valuable tool to assess the species-dependent uptake of metallopharmaceuticals into algal cells. *Chlamydomonas reinhardtii* algae were incubated for 24 h with four Gadolinium-based contrast agents (GBCAs) and $GdCl_3$. A species dependency towards the uptake of the tested Gd species was observed. Using single cell-ICP-MS, a Gd signal corresponding to single cell events was detected for $GdCl_3$ and the linear GBCAs Omniscan® (Gadodiamide, Gd-DTPA-BMA) and Magnevist® (Gadodiamide, Gd-DTPA). For the macrocyclic complexes Dotarem® (Gadoteric acid, Gd-DOTA) and Gadovist® (Gadobutrol, Gd-BT-DO3A), no such Gd signal was visible. Total Gd analysis via ICP-MS confirmed the presence of Gd in the cells only after incubation with $GdCl_3$ and the linear GBCAs, while only small amounts of Gd were detected for the incubations with macrocyclic GBCAs. Furthermore, the results showed that more Gd is bound to cell structures or macromolecules, while smaller amounts are present in the lysate. Using hydrophilic interaction liquid chromatography (HILIC)-ICP-MS, the soluble Gd species in the lysate were

Abbreviations: ACN, acetonitrile; Gd-DOTA, Dotarem®; GBCAs, gadolinium-based contrast agents; Gd-BT-DO3A, Gadovist®; HILIC, hydrophilic interaction liquid chromatography; ICP-MS, inductively coupled plasma-mass spectrometry; Gd-DTPA, Magnevist®; Gd-DTPA-BMA, Omniscan®; sc-ICP-MS, single cell-ICP-MS; SD, standard deviation; TAP, tris-acetate-phosphate buffer.

* Corresponding author.
E-mail address: uk@uni-muenster.de (U. Karst).

https://doi.org/10.1016/j.scitotenv.2023.166909
Received 16 June 2023; Received in revised form 5 September 2023; Accepted 6 September 2023
Available online 7 September 2023

analyzed to determine if the initial Gd complexes were still intact. Surprisingly, no intact GBCAs were detected in the lysates of any incubation solution, possibly due to a change in Gd speciation. Further research is needed to assess which Gd species are present in the lysate, while "free" Gd ions or adducts with cell constituents are the most likely explanation. This study highlights the need for species-dependent investigation of elements in aquatic organisms. Moreover, the uptake of linear GBCAs and their species alteration raises the question of a potential accumulation of Gd in the food chain.

1. Introduction

Pharmaceuticals moved into the center of attention as pollutants in the aqueous environment over the last decades due to their expanding use and the potential risk they pose (Mohan et al., 2021). In the 1990s, positive anomalies of the rare earth element Gd were detected in river waters in densely populated areas, caused by the increasing use of Gadolinium-based contrast agents (GBCAs) during magnetic resonance imaging (Bau and Dulski, 1996). Their contrast-enhancing effect is based on Gd^{3+} due to its paramagnetic properties, but it has to be administered in the form of stable complexes since the free ion is toxic (Lacampagne et al., 1994). Over the years, different GBCAs were developed, classified based on their complexing agent into ionic or non-ionic as well as linear or macrocyclic complexes. The stability of macrocyclic GBCAs in the body is higher compared to linear complexes, with ionic GBCAs being more stable than non-ionic (Idée et al., 2009). It was reported that after administration of linear GBCAs, especially for renally impaired patients, a Gd deposition in the body takes place. Recently, Gd was also detected in various organs of patients with normal renal function, e.g., in the brain (Grobner, 2006; Kanda et al., 2014). After their excretion, sewage treatment plants can remove only 10 % of GBCAs, which leads to a release of large amounts into the environment (Telgmann et al., 2012). As a result, GBCAs can be detected in many different surface waters (Birka et al., 2016; Horstmann et al., 2021; Lindner et al., 2013; Macke et al., 2021). Therefore, the uptake of Gd into aquatic organisms such as algae is of great interest to assess the risk of GBCAs and their potential reaction products towards the environment. At concentrations of 29.79 μmol/L, ionic Gd^{3+} led to a 50 % reduction in cell growth after 96 h for *Skeletona costatum* (Tai et al., 2010). Furthermore, toxic effects of Gd^{3+} on different sea urchin species were reported, which led to the inhibition of their skeleton development (Martino et al., 2017).

Nevertheless, the ecotoxicological risk of intact GBCAs is considered low due to their still low concentrations in the environment (Neubert et al., 2008). However, Bendakovská et al. reported the species-dependent biosorption of Gd on *Chlorella kessleri*, showing the highest bioconcentration factors for ionic Gd followed by the linear Multi-Hance® (Gadobenic acid, Gd-BOPTA) and the macrocyclic Dotarem® (Gadoteric acid, Gd-DOTA) (Bendakovská et al., 2019). Furthermore, a study assessing the uptake of Gd in different organisms via laser ablation-ICP-MS showed that Gd could be found in the intestine of *Daphnia magna* after feeding on single-celled algae that were previously exposed to Magnevist® (Gadopentetic acid, Gd-DTPA) (Lingott et al., 2016). Since the toxicity of Gd depends on the species present, it is important to assess differences in the behavior of Gd complexes and potential alteration in speciation after uptake into aquatic organisms. Single cell-ICP-MS (sc-ICP-MS) is a valuable tool to evaluate the elemental distribution in cells providing more insight into differences on a cellular basis and has been recently reviewed extensively by Yu et al. (2020). This analytical approach can be used to assess ecotoxicological influences of metal species (von der Au et al., 2020) and was applied, for example, to investigate the uptake of arsenate or Au nanoparticles into algal cells (Mavrakis et al., 2019; Merrifield et al., 2018).

For this study, sc-ICP-MS was used to investigate the species-dependent uptake of Gd complexes into *Chlamydomonas reinhardtii* algae as model organism. $GdCl_3$, the linear GBCAs Omniscan® (Gadodiamide, Gd-DTPA-BMA) and Gd-DTPA as well as the macrocyclic complexes Gadovist® (Gadobutrol, Gd-BT-DO3A) and Gd-DOTA were chosen in order to uncover the influence of the ligand in addition to the charge state of the complexes (see Fig. S1 in the supplementary file for the complex structures). Furthermore, a combination of total Gd analysis and speciation analysis based on hydrophilic interaction liquid chromatography-ICP-MS (HILIC-ICP-MS) was used to assess if intact GBCAs were present in the cell lysates after the incubation.

2. Materials and methods

2.1. Chemicals

The commercial injection solutions of the contrast agents Gd-DTPA-BMA (Omniscan®, 0,5 mmol/mL, GE Healthcare, Chicago, IL, USA), Gd-DOTA (Dotarem®, 0,5 mmol/mL, Guerbet, Roissy, France) and Gd-BT-DO3A (Gadovist®, 1.0 mmol/mL, Bayer Healthcare, Leverkusen, Germany) and Gd-DTPA (Magnevist®, 0,5 mmol/mLBayer Healthcare, Leverkusen, Germany) as well as $GdCl_3{\cdot}6\ H_2O$ (Thermo Fisher, Kandel, Germany) were used. $Na_2EDTA{\cdot}4H_2O$ and ammonium acetate were purchased from Sigma-Aldrich (Steinheim, Germany). Certified Ho and Gd ICP standard solutions (1000 mg/L) were purchased from SCP Science (Quebec, Canada) and Merck (Darmstadt, Germany), respectively. Nitric acid (65 %, AnalaR NORMAPUR®) was obtained from Merck (Darmstadt, Germany) and Acetonitrile (ACN, HiPerSolv CHROMANORM®) from VWR (Haasrode, Belgium). Doubly distilled H_2O was prepared using an Aquatron® A4000D water still purification system (Barloworld Scientific, Nemours, France), and for flow cytometry, water was purified by a Milli-Q Academic-System (18.2 MΩ cm, 0.2 μm filter, Merck, Molsheim, France).

For cell culture preparation, Tris-acetate-phosphate medium was prepared using $(NH_4)_6Mo_7O_{24}{\cdot}4\ H_2O$, $CuSO_4{\cdot}5H_2O$, H_3BO_3, K_3PO_4, NH_4Cl, $MgSO_4{\cdot}7\ H_2O$, $CaCl_2{\cdot}2H_2O$ Tris(hydroxymethyl)aminomethane (Tris), and $ZnSO_4{\cdot}7\ H_2O$ were obtained from Sigma-Aldrich (Steinheim, Germany) while $CoCl_2{\cdot}6\ H_2O$, $FeSO_4{\cdot}7H_2O$, $MnCl_2{\cdot}4H_2O$ were purchased from AppliChem (Darmstadt, Germany). Ethylenediaminetetraacetic acid ($Na_2EDTA{\cdot}2H_2O$), Hydrochloric acid (32 %, ROTIPURAN®) and acetic acid (96 %, ROTIPURAN®) from Carl Roth (Karlsruhe, Germany) were used.

2.2. Sample preparation

The cell culture preparation was performed at the Institute of Plant Biology and Biotechnology of the University Münster. Cells of the *C. reinhardtii* wild-type strain cc124 were grown photoheterotrophic under continuous light conditions in TAP medium (20 mmol/L Tris, 2.5 % 40× Beijerinck salts (*v*/v), 0.1 % trace elements solution with $Na_2EDTA{\cdot}2\ H_2O$ (134 μmol/L), and 1 mmol/L K_3PO_4 adjusted to pH 7 with acetic acid). All *C. reinhardtii* cultures were grown in acid-washed flasks to remove metal ions from the glassware before sterilizing them by autoclaving. For the incubation, the cells were adjusted to a density of $2{\bullet}10^6$ cells/mL, and separate incubation solutions with 10 μmol/L Gd-DTPA, Gd-DTPA-BMA, Gd-DOTA, Gd-BT-DO3A and $GdCl_3$, respectively, were prepared. All cell cultures were incubated for 24 h under the same light conditions as before. For every experimental section (sc-ICP-MS, total Gd analysis, HILIC-ICP-MS), separate cell incubation solutions were prepared.

For sc-ICP-MS analysis, six technical replicates were used. In order to

be analyzed via sc-ICP-MS, the incubation solutions were washed three times with ammonium acetate (10 mmol/L, pH 7) by centrifuging for 4 min at 1000*g* and resuspending in the same volume. The washing solutions were checked for remaining Gd content to ensure the number of washing steps was sufficient. For analysis via flow cytometry and sc-ICP-MS, the cell suspensions were diluted appropriately to a final cell density of approximately $5{\cdot}10^5$ cells/mL.

For total Gd and speciation analysis, three technical replicates were examined. The cell incubations of the four different GBCAs were washed three times with ammonium acetate (10 mmol/L, pH 7) by centrifuging for 3 min at 1000*g* and resuspending in the same volume. Afterwards, a nebulizer (BioNeb®, Glas-Col®, Terre Haute, IN, USA) was used twice at 2–3 bar with N_2 at 4 °C to break up the cells. The lysed cell incubation solutions were centrifuged for 10 min at 5000*g*. Then, the lysate was removed and kept for both speciation and total Gd analysis, and the residue was resuspended in 2 % nitric acid and heated to 80 °C for 120 min until it was dissolved completely.

For total Gd analysis, quantification was carried out via external calibration using Gd ICP standard solution at 2 % nitric acid in a concentration range from 0.5 μg/L to 25 μg/L with 1 μg/L Ho as internal standard. Both lysate and cell residue were diluted in 2 % nitric acid appropriately, and 1 μg/L Ho solution was added as internal standard.

For speciation analysis via HILIC-ICP-MS, the standards for Gd-EDTA, Gd-DTPA, Gd-DTPA-BMA, Gd-DOTA, and Gd-BT-DO3A, as well as the lysates were prepared in ACN and 50 mmol/L ammonium formate at pH 5.5 (70/30 *v*/v).

To investigate the influence of the EDTA and the TAP medium on the Gd species, standard solutions of Gd-DTPA, Gd-DTPA-BMA, Gd-DOTA, Gd-BT-DO3A, and $GdCl_3$ (10 μmol/L each) were incubated with a solution of 134 μmol/L EDTA and TAP medium for 24 h, respectively. Afterwards, the solutions were diluted appropriately and prepared in ACN and 50 mmol/L ammonium formate at pH 5.5 (70/30 v/v).

2.3. Instrumentation

Flow cytometry using a CytoFLEX (Beckman Coulter, Brea, CA, USA) was carried out in triplicate for 3 min per measurement for every cell suspension to determine the cell density in the incubation solutions. Afterward, the cell suspensions were introduced into a single quadrupole ICP-MS system (PlasmaQuant MS Elite, AnalytikJena, Jena, Germany) using a syringe pump at a flow rate of 10 μL/min. The ICP-MS system was equipped with a CytoNeb 50 nebulizer, a CytoSpray total consumption on-axis spray chamber (Elemental Scientific, Omaha, NE, USA), and a platinum sampler and skimmer. The RF power was set to 1550 W, and sheath gas flow was at 1.01 L/min and the nebulizer gas flow at 0.2 L/min for single-cell conditions. The isotopes ^{24}Mg and ^{158}Gd were subsequently monitored in six replicates each in 1 min intervals at a dwell time of 0.1 ms, with Mg serving as an endogenous reference element for the cells. The ion lens parameters were tuned daily to optimize the signal intensities.

The total Gd analysis was carried out using a single quadrupole ICP-MS system (Agilent 7700×, Agilent Technologies, Santa Clara, CA, USA) in combination with an autosampler (ASX-560, Teledyne CETAC Technologies, Omaha, NE, USA). The ICP-MS system was equipped with a platinum sampler with a copper core and a platinum skimmer with a brass core, and a Scott spray chamber was used. The RF power was at 1550 W, and the nebulizer flow was set to 1.1 L/min. The isotopes ^{158}Gd and ^{165}Ho were measured at a dwell time of 100 ms.

For speciation analysis, the same ICP-MS instrument set up was coupled to a Dionex UltiMate 3000 UHPLC system consisting of a degasser (SRD-3400), a pump (HPG-3200RS), an autosampler (WPS-3000TRS), and a column oven (TCC-3000RS) from Thermo Fisher Scientific (Germering, Germany). For these measurements, the RF power was at 1600 W, and the nebulizer gas was set to 0.29 L/min with an Ar/O_2 mixture (80/20) as option gas at 35 % to avoid the deposition of carbon from the organic eluent. The monitored isotope was ^{158}Gd at a dwell time of 100 ms. For the separation, an Accucore™ HILIC column (Thermo Fisher Scientific, Bremen, Germany) with dimensions of 50 mm × 2.1 mm and an inner diameter of 2.6 μm was used at a flow rate of 600 μL/min and 50 °C column oven temperature. As eluent, 70 % B (ACN) and 30 % A (ammonium formate, 50 mmol/L, pH 5.5) under isocratic conditions were used. The injection volume was set to 5 μL.

2.4. Single cell-ICP-MS data analysis

Time-resolved instrument raw data was analyzed using a software tool (spTool2) that is under development by Matthias Elinkmann, University of Münster. In this work, it was used to determine a detection threshold based on Poisson statistics (Currie, 1968) and to perform a split-event correction which combines adjacent dwell times with a signal reading above the threshold.

3. Results and discussion

3.1. Single cell-ICP-MS

In order to analyze *C. reinhardtii* algae with sc-ICP-MS, a cell density of approximately $5{\bullet}10^5$ cells/mL is beneficial to ensure the arrival of single cells at the detector (Laborda et al., 2013). Therefore, the cell density of the cell suspensions was determined prior to sc-ICP-MS measurements via flow cytometry. Furthermore, as a reference for the presence of cells in the solution, the endogenous element ^{24}Mg was also recorded in addition to the analyte isotope ^{158}Gd. The cell density detected via flow cytometry combined with the detection of the reference element Mg were used to ensure the analyzed cells were still intact.

In the time-resolved signals recorded with ICP-MS, Gd signal spikes induced by single cells were detected for *C. reinhardtii* incubations with $GdCl_3$, Gd-DTPA, and Gd DTPA-BMA, but not for Gd-DOTA and Gd-BT-DO3A (Fig. 1, time-resolved). A cell suspension not exposed to any Gd species served as control. Here, as expected, no significant number of Gd signal events was detected (see S2 in the supplementary file).

The histograms of the logarithmic intensities for the $GdCl_3$ and Gd-DTPA-BMA incubations show a distribution towards higher intensities compared to Gd-DTPA, suggesting a higher Gd concentration (Fig. 1). For Gd-DTPA, the median logarithmic intensity is 1.76, while the mean logarithmic intensity is 1.92. This shows that for Gd-DTPA, a distribution towards higher intensities is detected, with the maximum close to the background. In the case of the other linear GBCA, namely Gd-DTPA-BMA, a more symmetric distribution of the logarithmic intensity is obtained, with median and mean logarithmic intensity being at 2.21 and 2.27, respectively. For the macrocyclic GBCAs Gd-DOTA and Gd-BT-DO3A, as expected from the time-resolved visualization, no significant Gd event distribution is present. The background signals for the macrocyclic GBCAs are lower compared to the incubation solutions of $GdCl_3$ and the linear GBCAs. This indicates that washing of the cell suspensions prior to the analysis was sufficient and no Gd from the incubation is present anymore.

Table 1 contains the mean cell density of the incubation solutions as determined via flow cytometry and the number of events detected via sc-ICP-MS for the cell reference element Mg and the analyte Gd. The percentage of cells inducing a signal during ICP-MS analysis was calculated based on the cell density and event rate. Green algae contain high levels of Mg which is present in the chlorophyll complex. Therefore, Mg was chosen as a cell signal marker. The ratio of the event rate based on ^{24}Mg and the rate of cells delivered to the nebulizer, which can be calculated from cell density and sample flow rate, is equal to the transport efficiency. The overall transmission rate for the reference nuclide ^{24}Mg, and therefore the overall cell transport efficiency, in all cell suspensions is 58 % ± 11 %.

The mean signal intensity for ^{158}Gd is corresponding to the mean concentration of Gd per cell. It is highest for $GdCl_3$, followed by Gd-DTPA-BMA and Gd-DTPA with 513 ± 85 cts, 367 ± 22 cts and 174 ±

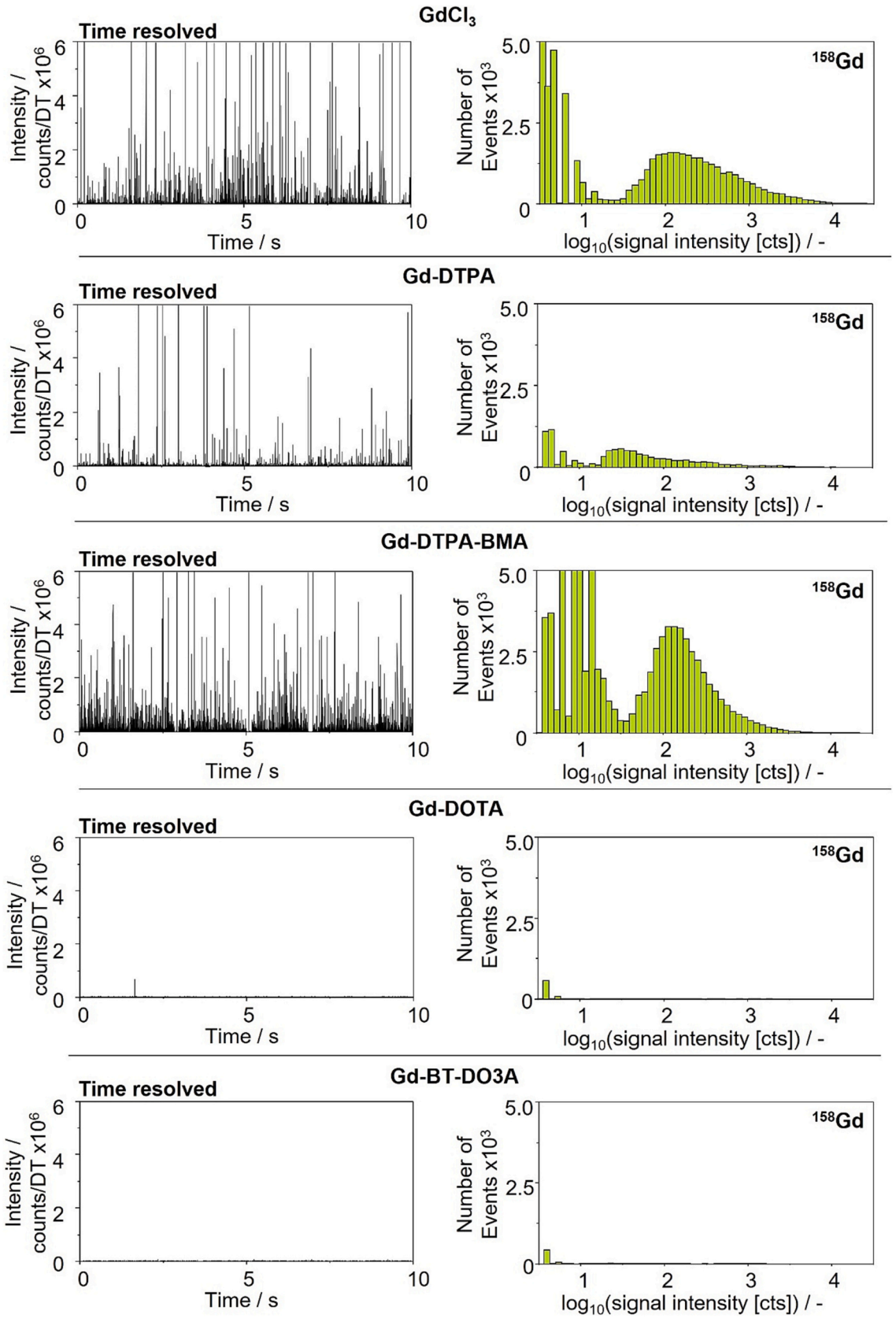

Fig. 1. Transient signals (left) and respective histograms for the common logarithm of the intensities (right) for the incubations of *C. reinhardtii* with GBCAs and $GdCl_3$.

Table 1
Mean cell density measured via flow cytometry, the number of cell events per mL detected via sc-ICP-MS and the calculated percentage of cells inducing a particle event for ^{24}Mg, including the respective standard deviations (SD). The mean event intensity for ^{24}Mg and ^{158}Gd is shown.

Gd species	Mean cell density/10^5 cells/mL	sc-ICP-MS/ 10^5 events/ mL	Cells inducing event/%	Mean intensity/ cts	
		Mg	Mg	Mg	Gd
Control	5.6 ± 0.2	2.8 ± 0.2	57 ± 5	754 ± 261	136 ± 24
$GdCl_3$	3.8 ± 0.3	2.1 ± 0.2	54 ± 9	2613 ± 319	513 ± 85
Gd-DTPA-BMA	5.2 ± 0.2	1.9 ± 0.1	40 ± 10	1703 ± 330	367 ± 22
Gd-DTPA	4.2 ± 0.2	2.7 ± 0.1	68 ± 4	2136 ± 491	174 ± 31
Gd-DOTA	4.7 ± 0.8	3.2 ± 0.3	73 ± 17	1572 ± 351	163 ± 66
Gd-BT-DO3A	5.2 ± 0.3	2.8 ± 0.3	59 ± 9	1249 ± 131	146 ± 70

31 cts, respectively. For Gd-DOTA and Gd-BT-DO3A, the mean intensities of 163 ± 66 cts and 146 ± 70 cts are comparable to Gd-DTPA. However, as is visible in Fig. 1, the amount of detected signals is low and the relative standard deviation of the mean intensities are high with 41 % and 48 %, respectively. In addition, the mean signal intensities of Gd-DTPA, Gd-DOTA and Gd-BT-DO3A are close to the mean signal intensities detected for the control sample.

Comparing the two linear GBCAs, Gd-DTPA interacts with the cells to a lower degree than Gd-DTPA-BMA. This corresponds to the respective histograms of the Gd intensity distributions indicating lower concentrations of Gd in the detected cells for Gd-DTPA.

Using sc-ICP-MS, it is not possible to determine whether Gd that was taken up by the cells or is bound to the outer cell walls of the algae. Therefore, the total Gd content in the lysate and in the cell residue was compared.

3.2. Total Gd analysis

The cells were opened with a nebulizing cell disruption system to carry out total Gd analysis of the lysate and the cell residue to differentiate between free Gd species and Gd bound to macromolecules or cell structures (Fig. 2). The LOD and LOQ for the Gd quantification, determined based on the standard deviation of the response and the slope following the ICH guideline Q2(R1) (ICH Expert Working Group, 2005), were found to be 0.3 ng/L and 1.0 ng/L, respectively. With regard to the Gd amount per cell, the LOQ is corresponding to a concentration of $0.03{\cdot}10^{-16}$ g Gd/cell for the lysate and $0.01{\cdot}10^{-16}$ g Gd/cell for the cell residue.

For the control sample and the macrocyclic Gd-DOTA, no Gd in the lysate or bound to the cell residue could be detected. For the macrocyclic Gd-BT-DO3A, only $0.59 \pm 0.21{\cdot}10^{-16}$ g Gd/cell and $0.29 \pm 0.02{\cdot}10^{-16}$ g Gd/cell were detected in lysate and cell residue, respectively. However, it should be noted that while the calculated concentrations for Gd per cell are higher than the LOQ, the concentrations are below the lowest calibration point.

In case of the lysates of the incubations with linear GBCAs, $5.6 \pm 0.4{\cdot}10^{-16}$ g Gd/cell for Gd-DTPA and $9.6 \pm 0.4{\cdot}10^{-16}$ g Gd/cell for Gd-DTPA-BMA were found. In the cell residue, $11 \pm 0.2{\cdot}10^{-16}$ g Gd/cell are present in the Gd-DTPA incubation and $17 \pm 0.2{\cdot}10^{-16}$ g Gd/cell for Gd-DTPA-BMA. Therefore, the observed total Gd analysis confirms higher uptake of Gd-DTPA-BMA compared to the incubations with Gd-DTPA. Approximately 70 % more Gd was detected in the lysate and 50 % more was found in the residue for Gd-DTPA-BMA compared to Gd-DTPA. A possible explanation could be the ionic character and the higher thermodynamic stability of Gd-DTPA in contrast to the non-ionic Gd-DTPA-BMA (Hao et al., 2012). Furthermore, these results confirm that no or only a small amount of Gd is taken up by the cells when exposed to macrocyclic GBCAs.

For $GdCl_3$, $500 \pm 1{\cdot}10^{-16}$ g Gd/cell cells were detected in the lysate compared to $1300 \pm 5{\cdot}10^{-16}$ g Gd/cell in the residue. Therefore, the uptake of $GdCl_3$ was much higher than for the GBCAs. However, similar to the linear GBCAs, more Gd was found in the cell residue than in the lysate.

For $GdCl_3$, the Gd amount in the cell residue is 2.6 times the amount in the lysate, while for the linear GBCAs, the factors are 1.8 for Gd-DTPA-BMA and 2.0 for Gd-DTPA.

For the macrocyclic Gd-BT-DO3A, where small amounts of Gd were quantified, two times more Gd was present in the lysate than in the cell residue.

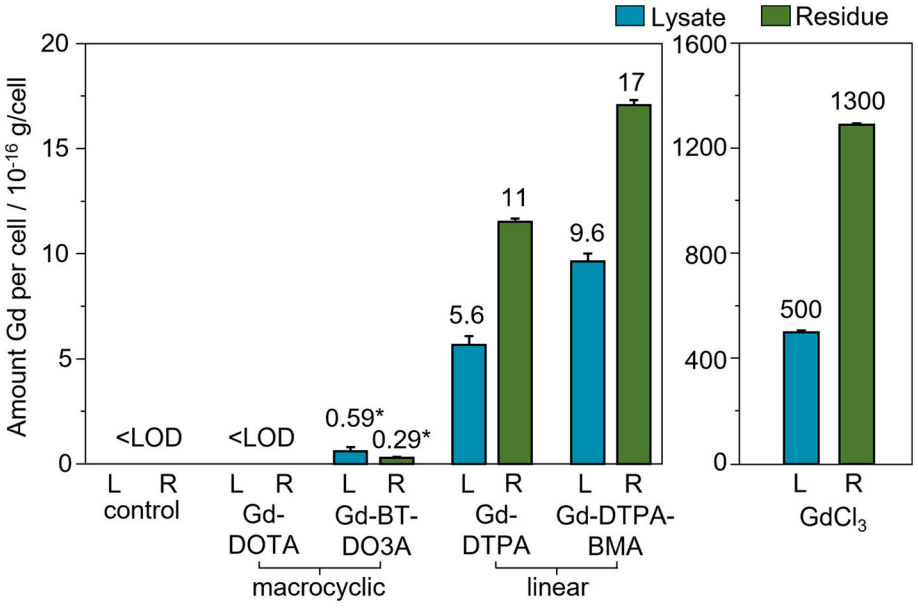

Fig. 2. Amount of Gd per 10^7 cells in the lysate and cell residue for the incubation solutions of *C. reinhardtii* with Gd-DOTA, Gd-BT-DO3A, Gd-DTPA, Gd-DTPA-BMA, and $GdCl_3$ determined with ICP-MS. Values marked with an asterisk (*) were outside the calibration range.

This suggests that $GdCl_3$ and the linear GBCAs are more likely to be bound to cell structures such as cell walls, cell organelles, or macromolecules like proteins. The results correspond to the results of the sc-ICP-MS experiments, where a trend of highest Gd concentrations per cell for the incubation with $GdCl_3$, followed by Gd-DTPA-BMA and Gd-DTPA, was detected.

Since linear GBCAs are more likely to transmetalate and release Gd^{3+} than the macrocyclic GBCAs (Runge, 2018), this is a possible explanation for the opposed behavior of the GBCAs and the similarity of linear GBCAs to the behavior of $GdCl_3$. Since the residue contains cell organelles or proteins as well as cell walls, it is not possible to determine whether Gd is sorbed on the outer cell walls or bound to macromolecular structures inside the algae.The results are in accordance with the findings of earlier studies showing the highest biosorption of ionic Gd on the algae *C. kessleri* followed by the linear Gd-BOPTA and the macrocyclic Gd-DOTA (Bendakovská et al., 2019). However, they reported a concentration of approximately 30 mg/kg Gd in the cells for Gd-DOTA, which contradicts the results obtained via sc-ICP-MS showing no uptake of this Gd complex at all. This could be due to the higher initial Gd species concentrations by a factor of 10 used for the experiments.

The Gd present in the lysate after centrifugation represents the soluble part in the cells, which could be free Gd^{3+}, the intact linear GBCAs, or soluble Gd adducts with cell constituents of low molecular weight. Therefore, HILIC-ICP-MS measurements of the lysate were carried out to obtain information about the present Gd species.

3.3. HILIC-ICP-MS analysis

Fig. 3 shows an overlay of the chromatograms of the GBCA standards (A) and the chromatograms recorded for the cell lysates of the incubation solutions (B). Here, the separation of the four GBCAs was achieved under isocratic conditions in 2.5 min. Since no mixtures of the GBCAs were expected in the sample solutions, no baseline separation of the Gd species was required. The analysis of the lysates that were obtained by disrupting the cells through nebulization showed that no intact GBCAs were present in each of the analyzed incubations. Since Gd was found in the lysates of the incubations with linear GBCAs, a change in the initial Gd speciation occurred. Free Gd^{3+} cannot be analyzed using this method since these uncomplexed metal ions tend to adsorb on the stationary phase. Therefore, further experiments are necessary to elucidate whether the change in speciation is due to a release of Gd^{3+} or caused by adduct formation with other cell components that were not detected with this method.

TAP medium was used to cultivate the cells, containing essential metal elements providing optimal conditions for algal cell growth. EDTA is added as a complexing agent to TAP medium to prevent the metal ions from precipitating and remain bioavailable for the cells. To examine whether the presence of EDTA is influencing the Gd speciation, incubation experiments with the GBCAs and $GdCl_3$ were carried out with EDTA as well as TAP medium without cells. These solutions were analyzed via HILIC-ICP-MS. The results show that even though EDTA can alter the Gd speciation present, especially in the case of ionic Gd and the linear GBCAs, this effect is negligible when the Gd species are incubated with the TAP medium without cells (see Fig. 4). For the cell suspensions in TAP medium, this effect is even less pronounced.

4. Conclusion

This study showed that sc-ICP-MS is a valuable tool for investigating the uptake of metallopharmaceuticals in cells. Differences in the uptake into *C. reinhardtii* algae for different Gd species were observed. The highest degree of interaction occurred for $GdCl_3$, followed by linear GBCAs, with the non-ionic Gd-DTPA-BMA showing a higher reactivity than the ionic Gd-DTPA. For the macrocyclic GBCAs, no uptake into the algal cell was detected.

Total Gd analysis with ICP-MS showed that while Gd is present in the cell lysate of the incubations with $GdCl_3$ and linear GBCAs, it is more likely to bind to macromolecular cell structures or proteins. Using HILIC-ICP-MS to elucidate the Gd species present in the lysate, no intact GBCAs were detected. Hence, a change in speciation of the linear GBCAs took place, with "free" Gd^{3+} or low molecular weight adducts with cell components as a possible explanation. These results highlight that it is

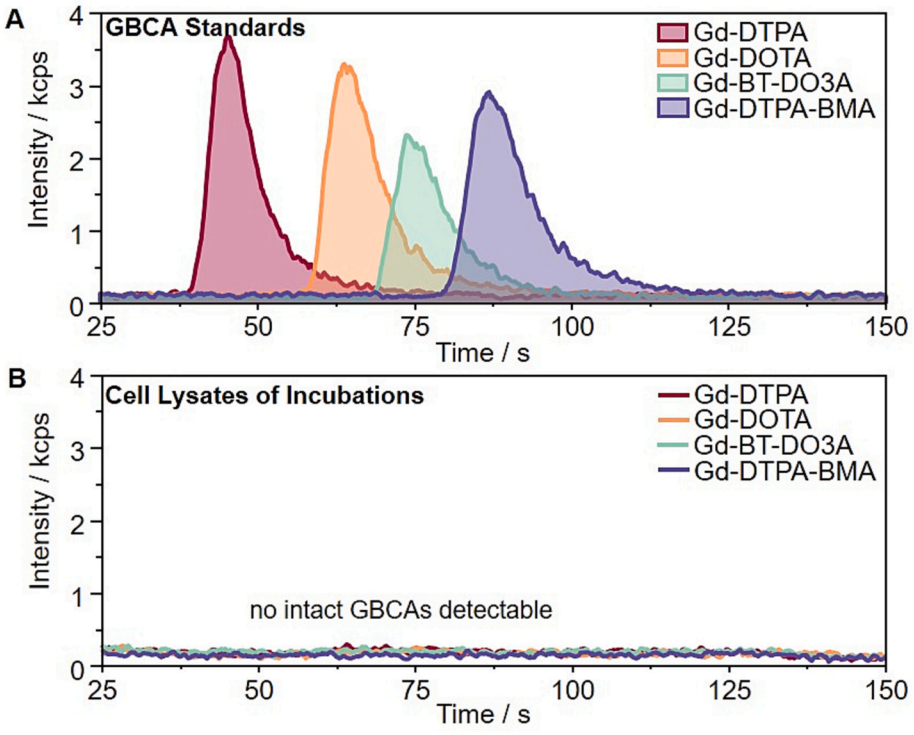

Fig. 3. Overlay of HILIC-ICP-MS chromatograms of the GBCA standards (A) and the respective lysates of the GBCA cell incubations (B).

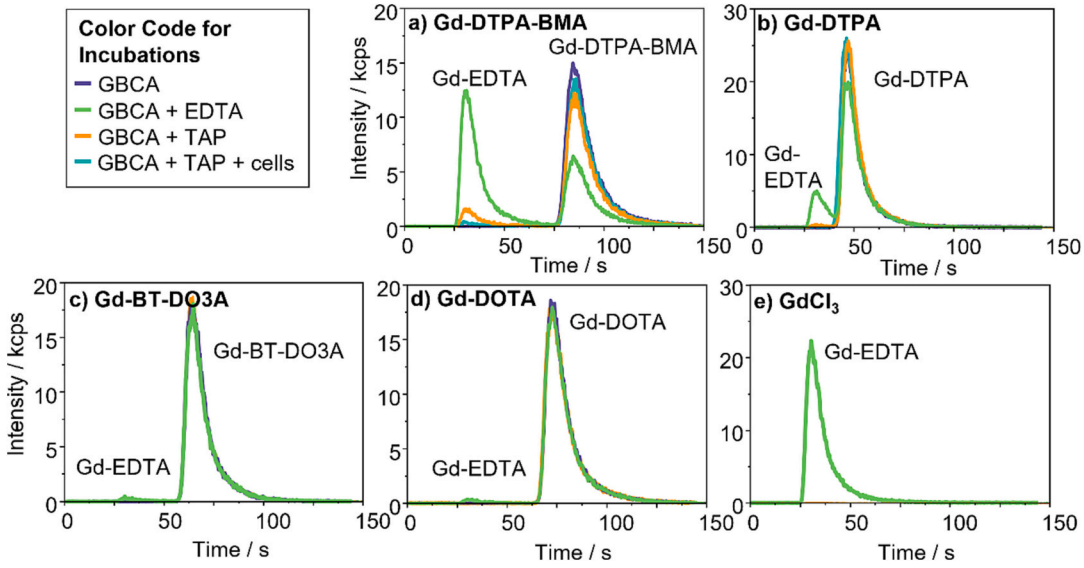

Fig. 4. Chromatograms of the ^{158}Gd signal of the incubation solutions with EDTA, TAP and cell cultures with Gd-DTPA-BMA (a), Gd-DTPA (b), Gd-BT-DO3A (c), Gd-DOTA (d) and $GdCl_3$ (e). Furthermore, the chromatograms of the GBCAs without any additional compounds are shown as reference.

important to consider the Gd speciation when investigating GBCAs in the environment since the behavior of ionic Gd, linear and macrocyclic complexes can be very different. Furthermore, the uptake of linear GBCAs raises the question of the potential accumulation of Gd in the food chain. Since Gd ions are toxic, the Gd species in the lysate should be topic of further research to assess potential adverse effects posed to algae or other aquatic organisms.

CRediT authorship contribution statement

Karolin Sommer: Conceptualization, Data curation, Formal analysis, Investigation, Methodology, Visualization, Writing – original draft. **Sarah Reuter:** Investigation, Methodology, Visualization, Writing – review & editing. **Matthias Elinkmann:** Data curation, Formal analysis, Investigation, Methodology, Visualization, Writing – review & editing. **Alexander Köhrer:** Data curation, Formal analysis, Investigation, Methodology, Visualization, Writing – review & editing. **C. Derrick Quarles:** Resources, Methodology, Validation, Writing – review & editing. **Michael Hippler:** Conceptualization, Methodology, Validation, Resources, Writing – review & editing, Supervision. **Uwe Karst:** Conceptualization, Methodology, Validation, Resources, Writing – review & editing, Supervision.

Declaration of competing interest

The authors declare that they have no known competing financial interests or personal relationships that could have appeared to influence the work reported in this paper.

Data availability

Data will be made available on request.

Acknowledgements

A Ph.D. scholarship to Karolin Sommer by the German Federal Environmental Foundation (DBU, Osnabrück, Germany) is gratefully acknowledged.

Appendix A. Supplementary data

Supplementary data to this article can be found online at https://doi.org/10.1016/j.scitotenv.2023.166909.

References

Bau, M., Dulski, P., 1996. Anthropogenic origin of positive gadolinium anomalies in river waters. Earth Planet. Sci. Lett. 143, 245–255. https://doi.org/10.1016/0012-821X(96)00127-6.

Bendakovská, L., Krejčová, A., Weidlich, T., 2019. Sorption and biosorption of Gd-based contrast agents in the water environment. Chem. Pap. 73, 2995–3003. https://doi.org/10.1007/s11696-019-00751-8.

Birka, M., Wehe, C.A., Hachmöller, O., Sperling, M., Karst, U., 2016. Tracing gadolinium-based contrast agents from surface water to drinking water by means of speciation analysis. J. Chromatogr. A 1440, 105–111. https://doi.org/10.1016/j.chroma.2016.02.050.

Currie, L.A., 1968. Limits for qualitative detection and quantitative determination: application to radiochemistry. Anal. Chem. 40, 586–593. https://doi.org/10.1021/ac60259a007.

Grobner, T., 2006. Gadolinium – a specific trigger for the development of nephrogenic fibrosing dermopathy and nephrogenic systemic fibrosis? Nephrol. Dial. Transplant. 21, 1104–1108. https://doi.org/10.1093/ndt/gfk062.

Hao, D., Ai, T., Goerner, F., Hu, X., Runge, V.M., Tweedle, M., 2012. MRI contrast agents: basic chemistry and safety. J. Magn. Reson. Imaging 36, 1060–1071. https://doi.org/10.1002/jmri.23725.

Horstmann, M., Gonzalez De Vega, R., Bishop, D.P., Karst, U., Doble, P.A., Clases, D., 2021. Determination of gadolinium MRI contrast agents in fresh and oceanic waters of Australia employing micro-solid phase extraction, HILIC-ICP-MS and bandpass mass filtering. J. Anal. At. Spectrom. 36, 767–775. https://doi.org/10.1039/d0ja00493f.

ICH Expert Working Group, 2005. ICH Harmonised Tripartite Guideline: Validation of Analytical Procedures: Text and Methodology Q2(R1).

Idée, J.-M., Port, M., Robic, C., Medina, C., Sabatou, M., Corot, C., 2009. Role of thermodynamic and kinetic parameters in gadolinium chelate stability. J. Magn. Reson. Imaging 30, 1249–1258. https://doi.org/10.1002/jmri.21967.

Kanda, T., Ishii, K., Kawaguchi, H., Kitajima, K., Takenaka, D., 2014. High signal intensity in the dentate nucleus and globus pallidus on images: relationship with increasing cumulative dose of a gadolinium-based contrast material. Radiology 270, 834–841. https://doi.org/10.1148/radiol.13131669.

Laborda, F., Jiménez-Lamana, J., Bolea, E., Castillo, J.R., 2013. Critical considerations for the determination of nanoparticle number concentrations, size and number size distributions by single particle ICP-MS. J. Anal. At. Spectrom. 28, 1220–1232. https://doi.org/10.1039/C3JA50100K.

Lacampagne, A., Gannier, F., Argibay, J., Garnier, D., Le Guennec, J.Y., 1994. The stretch-activated ion channel blocker gadolinium also blocks L-type calcium channels in isolated ventricular myocytes of the guinea-pig. Biochim. Biophys. Acta Biomembr. 1191, 205–208. https://doi.org/10.1016/0005-2736(94)90250-X.

Lindner, U., Lingott, J., Richter, S., Jakubowski, N., Panne, U., 2013. Speciation of gadolinium in surface water samples and plants by hydrophilic interaction chromatography hyphenated with inductively coupled plasma mass spectrometry. Anal. Bioanal. Chem. 405, 1865–1873. https://doi.org/10.1007/s00216-012-6643-x.

Lingott, J., Lindner, U., Telgmann, L., Esteban-Fernández, D., Jakubowski, N., Panne, U., 2016. Gadolinium-uptake by aquatic and terrestrial organisms-distribution determined by laser ablation inductively coupled plasma mass spectrometry. Environ Sci Process Impacts 18, 200–207. https://doi.org/10.1039/c5em00533g.

Macke, M., Quarles, C.D., Sperling, M., Karst, U., 2021. Fast and automated monitoring of gadolinium-based contrast agents in surface waters. Water Res. 207, 117836 https://doi.org/10.1016/J.WATRES.2021.117836.

Martino, C., Bonaventura, R., Byrne, M., Roccheri, M., Matranga, V., 2017. Effects of exposure to gadolinium on the development of geographically and phylogenetically distant sea urchins species. Mar. Environ. Res. 128, 98–106. https://doi.org/10.1016/j.marenvres.2016.06.001.

Mavrakis, E., Mavroudakis, L., Lydakis-Simantiris, N., Pergantis, S.A., 2019. Investigating the uptake of arsenate by chlamydomonas reinhardtii cells and its effect on their lipid profile using single cell ICP-MS and Easy Ambient Sonic-Spray Ionization-MS. Anal. Chem. 91, 9590–9598. https://doi.org/10.1021/acs.analchem.9b00917.

Merrifield, R.C., Stephan, C., Lead, J.R., 2018. Quantification of Au nanoparticle biouptake and distribution to freshwater algae using single cell - ICP-MS. Environ. Sci. Technol. 52, 2271–2277. https://doi.org/10.1021/acs.est.7b04968.

Mohan, H., Rajput, S.S., Jadhav, E.B., Sankhla, M.S., Sonone, S.S., Jadhav, S., Kumar, R., 2021. Ecotoxicity, occurrence, and removal of pharmaceuticals and illicit drugs from aquatic systems. Biointerface Res. Appl. Chem. 11, 12530–12546. https://doi.org/10.33263/BRIAC115.1253012546.

Neubert, C., Länge, R., Steger-Hartmann, T., 2008. Gadolinium containing contrast agents for magnetic resonance imaging (MRI). In: Fate of Pharmaceuticals in the Environment and in Water Treatment Systems. CRC Press, Boca Raton, pp. 101–118.

Runge, V.M., 2018. Dechelation (transmetalation): consequences and safety concerns with the linear gadolinium-based contrast agents, in view of recent health care rulings by the EMA (Europe), FDA (United States), and PMDA (Japan). Investig. Radiol. 53, 571–578. https://doi.org/10.1097/RLI.0000000000000507.

Tai, P., Zhao, Q., Su, D., Li, P., Stagnitti, F., 2010. Biological toxicity of lanthanide elements on algae. Chemosphere 80, 1031–1035. https://doi.org/10.1016/j.chemosphere.2010.05.030.

Telgmann, L., Wehe, C.A., Birka, M., Künnemeyer, J., Nowak, S., Sperling, M., Karst, U., 2012. Speciation and isotope dilution analysis of gadolinium-based contrast agents in wastewater. Environ. Sci. Technol. 46, 11929–11936. https://doi.org/10.1021/es301981z.

von der Au, M., Borovinskaya, O., Flamigni, L., Kuhlmeier, K., Büchel, C., Meermann, B., 2020. Single cell-inductively coupled plasma-time of flight-mass spectrometry approach for ecotoxicological testing. Algal Res. 49, 101964 https://doi.org/10.1016/j.algal.2020.101964.

Yu, X., He, M., Chen, B., Hu, B., 2020. Recent advances in single-cell analysis by inductively coupled plasma-mass spectrometry: a review. Anal. Chim. Acta 1137, 191–207. https://doi.org/10.1016/j.aca.2020.07.041.